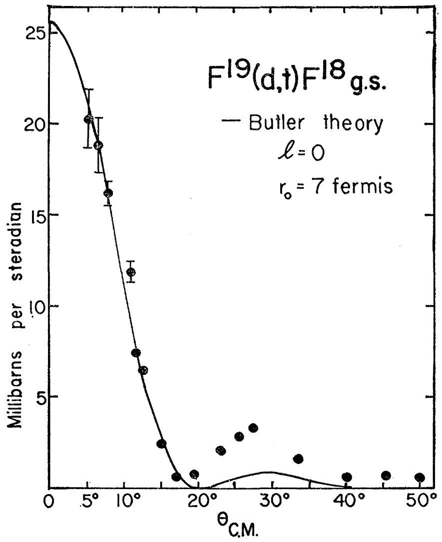

FIG. 5. Angular distribution of the reaction $F^{19}(d,t)F^{18}$ g.s. with 14.8-Mev deuterons.

analysed, were detected in Kodak NTB, 50μ thick, nuclear emulsions. The angular acceptance was limited to 1°.

The experimental angular distribution is shown in Fig. 5 together with an $l=0$ Butler curve using $r_0=7$ fermis. The absolute cross section was calculated by comparison with measurements of the $C^{12}(d,p)C^{13}$ g.s. reaction using the same Teflon target. The cross section of that reaction has been previously measured to $\pm 20\%$ at this laboratory.[13] The result of the experiment in terms of the reduced width is presented in Table I, and its comparison with the corresponding (p,d) reaction is discussed in Sec. III.

ACKNOWLEDGMENTS

The author wishes to express her gratitude to N. Austern and J. B. French for guidance and many discussions throughout the work. She is also grateful to several people for help and encouragement, mainly to A. J. Allen, J. R. Cameron, and E. W. Hamburger.

PHYSICAL REVIEW VOLUME 118, NUMBER 5 JUNE 1, 1960

Conversion, *K*-Auger, and *L*-Auger Spectra of Hg^{199}†

J. C. NALL, Q. L. BAIRD,* AND S. K. HAYNES‡
Department of Physics, Vanderbilt University, Nashville, Tennessee
(Received December 17, 1959)

The high resolution of the spectrometer made possible the detailed study of K, L, M, $N+O$ conversion lines and the K- and L-Auger spectra of Au^{199} with the following results (here ω and a are the fluorescence and Auger yields and f_{ij} is the Coster-Kronig transfer probability): K-Auger lines, $\omega_K=0.952\pm0.003$, $KLL:KLX:KXY=1.00:0.496\pm0.015:0.094\pm0.003$, and $KL_1L_1:KL_1L_2:KL_1L_3:KL_2L_2:KL_2L_3:KL_3L_3=1.00:1.32\pm0.1:0.85\pm0.06:0.40\pm0.03:1.28\pm0.08:0.76\pm0.05$; L-Auger lines, $LMM:LMX:LXY=1.00:0.30\pm0.03:0.015\pm0.004$, and $a_L=0.590\pm0.04$, $\omega_L=0.410\pm0.04$, $a(L_1)=0.16\pm0.02$, $a(L_2)=0.46\pm0.04$, $\omega(L_2)=0.32\pm0.03$, and Coster-Kronig yields, $f(L_2L_3X)=0.22\pm0.04$, $f(L_1L_2X)+f(L_1L_3X)=0.74\pm0.04$. In addition considerable detail was obtained on the KLX and L-Auger fine structure. The results of all of the known L-Auger yield work since 1952 have been tabulated in this paper.

The conversion line results are compared and combined with those of two other groups to give an optimum set of relative intensities.

From these are obtained for the 51-kev transition, $\alpha(L_1):\alpha(L_2):\alpha(L_3):\alpha(M):\alpha(N):\alpha(O)=1.00:0.087\pm0.010:0.012\pm0.007:0.212\pm0.04:0.068\pm0.005:0.016\pm0.001$; 156-kev transition, $\alpha(K):\alpha(L_1):\alpha(L_2):\alpha(L_3):\alpha(M):\alpha(N+O)=1.00:0.144\pm0.015:0.830\pm0.028:0.586\pm0.018:0.418\pm0.017:0.107\pm0.005$; 209-kev transition, $\alpha(K):\alpha(L_1):\alpha(L_2):\alpha(L_3):\alpha(M):\alpha(N+O)=1.00:0.155\pm0.005:0.029\pm0.003:0.0085\pm0.0003:0.050\pm0.006:0.0130\pm0.004$, where α is the internal conversion coefficient.

In addition, by use of Rose's Tables the 51-kev transition was determined to be $3.3\pm1\times10^{-4}$ $E2$, and the 209-kev transition 0.113 ± 0.01 $E2$, and the $E2$ assignment of the 158-kev transition was confirmed to better than 1%. The relative gamma-ray intensities are 209 kev:51 kev:158 kev$=1.000:0.045\pm0.002:4.59\pm0.23$.

I. INTRODUCTION

ALTHOUGH the electron spectrum of the radionuclide Au^{199} has been studied with various types of spectrometers, discrepancies exist in the conversion line results and the K- and L-Auger lines have never been studied with high resolution. Therefore, when the Vanderbilt University, iron-free $\pi\sqrt{2}$ spectrometer became operational, a thorough study of the electron line spectrum of Au^{199} from 5 kev to 210 kev was undertaken. The continuous beta-ray spectrum was studied only sufficiently to establish a baseline for the various line spectra.

The well established decay scheme of Au^{199} is shown in Fig. 1.[1–3] The energies of the upper two gamma rays have recently been measured to be 209.17+0.12 kev and 158.27±0.35 kev.[4] The character of the 158-kev

† Supported by a grant from the National Science Foundation.
* Now at Argonne National Laboratory, Lemont, Illinois.
‡ Now at Michigan State University, East Lansing, Michigan.

[1] P. Sherk and R. Hill, Phys. Rev. **83**, 1097 (1951).
[2] P. J. Cressman and R. G. Wilkinson, Phys. Rev. **109**, 872 (1958).
[3] G. Bäckström, O. Bergman, and J. Burde, Nuclear Phys. **7**, 263 (1958).
[4] M. P. Avotina and O. I. Sumbaev, *Izvest. Akad. Nauk. S.S.S.R.* Ser. Fiz. **22**, 879 (1958).

transition has been shown to be nearly pure $E2$ while the 51- and 209-kev transitions are $M1$ with small mixtures of $E2$. The chief purpose of the conversion line study was to check certain discrepancies between Cressman and Wilkinson[2] and Bäckström *et al.*[3] for the relative subshell conversion intensities, to re-evaluate the mixing ratios of the 51- and 209-kev transitions, and to check the accuracy of recent recalculations of Internal Conversion coefficients, taking account of the effect of finite nuclear size.[5–7] These results are given and discussed in Sec. IVA.

Of the several K-Auger spectra around $Z=80$ which have been studied with high resolution, all have been observed with photographic spectrometers.[8] Moreover, the low value of the K-Auger yield for large Z has made all intensity measurements somewhat inaccurate. In view of the high intensity of the continuous beta-ray spectrum in the K-Auger region, Au^{199} is not ideal for such measurements, but it was felt that because of the fairly high resolution available, increased accuracy could be obtained both in global K-Auger yield and in knowledge of the K-Auger fine structure by a careful study of this region of the spectrum. The results of this study are given in Sec. IVB.

The study of L-Auger spectra is more difficult than K-Auger spectra for several reasons. (1) Their energy is much lower which necessitates use of very thin

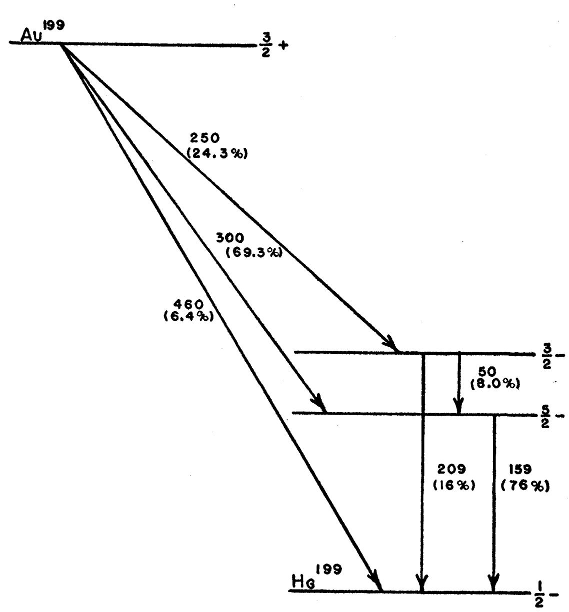

FIG. 1. The decay scheme of Au^{199}.

sources and detectors with 100% or known response at low energies. (2) Many more lines are present than in K-Auger spectra, therefore, line separation is difficult and maximum resolution is necessary. (3) Subshell L-Auger and L-fluorescence yields are strongly affected by the Coster-Kronig effect which transfers holes from one L subshell to another.

As a result of the Coster-Kronig effect, one has the following equations for the three L subshells instead of the simple equation $\omega+a=1$ which holds for the K-shell yields:

$$\omega_1+a_1+f_{12}+f_{13}=1, \quad (1)$$

$$\omega_2+a_2+f_{23}=1, \quad (2)$$

$$\omega_3+a_3=1, \quad (3)$$

ω_i and a_i are the fluorescence yield and Auger yield, respectively, of the ith subshell and f_{ij} is the Coster-Kronig probability of transfer of a hole from the ith subshell to the jth subshell. The chief purpose of L-Auger spectroscopy is the determination of the 9 quantities given in Eqs. (1) to (3). Work done prior to 1952 has been tabulated by Burhop.[9] It is evident that the general agreement was poor.

Ross *et al.*,[10] were the first to determine the total yields and the nine subshell and Coster-Kronig yields for an element. Actually four total yields were given, the ω_L and a_L for fluorescent excitation and the two for internal conversion excitation. They chose Bi because a large amount of work of various kinds had been done using RaD which decays by beta emission to Bi^{210}. In particular, L-Auger spectra had been obtained by Kobayashi[11] and Bashilov *et al.*[12] Also several investigators had used ThB which has Bi^{212} as one of its products. Ross *et al.* have compiled and interpreted these data to determine the Bi yields (Table VI). Recent work, with RaD as a source, has been carried out by Tousset and Moussa.[13] These investigators used an iron-free, double-focusing spectrometer and have obtained values for the total and some subshell and Coster-Kronig yields of Bi^{210}. Their results are also given in Table V.

Additional determinations of the relative Auger-line intensities of Bi have been furnished by investigators who have used ThB in equilibrium with its decay products. The L-Auger spectra of Tl^{208} and Bi^{212} were studied by Moussa and Bellicard[14] and Bellicard[15] by means of an iron-free, double-focusing instrument. Burde and Cohen[16] have employed a thin magnetic-lens

[5] L. A. Sliv and M. A. Listengarten, Zhur. Eksp. i Teoret. Fiz. **22**, 29 (1952).
[6] L. A. Sliv and I. M. Band, [translation: Leningrad Physico-Technical Institute Report, 1956 Report 57ICCKl, Physics Department, University of Illinois, Urbana, Illinois (unpublished)].
[7] M. E. Rose, *Internal Conversion Coefficients* (North-Holland Publishing Company, Amsterdam, 1958).
[8] I. Bergström, in *Beta- and Gamma-Ray Spectroscopy*, edited by Kai Siegbahn (North-Holland Publishing Company, Amsterdam 1955), p. 631.
[9] E. H. S. Burhop, *The Auger Effect and Other Radiationless Translations* (Cambridge University Press, New York, 1952).
[10] M. A. S. Ross, A. J. Cochran, J. Hughes, and N. Feather, Proc. Phys. Soc. (London) **A68**, 612 (1955).
[11] Y. Kobayashi, J. Phys. Soc. Japan **8**, 440 (1953).
[12] A. A. Bashilov, B. S. Dzhelepov, and L. S. Chervinskaya, Izvest Akad. Nauk. S. S. S. R. **17**, 428 (1953).
[13] J. Tousset and A. Moussa, J. phys. radium **19**, 39 (1958).
[14] A. Moussa and J. B. Bellicard, Compt. rend. **242**, 1156 (1956).
[15] J. B. Bellicard, Ann. Phys. **2**, 419 (1957).
[16] J. Burde and S. G. Cohen, Phys. Rev. **104**, 1085 (1956).

spectrometer and coincidence techniques to determine a_1, a_2, a_3, f_{12}, and f_{13}. They have made the approximations that the yields are the same for Tl and Bi and that the Coster-Kronig yield f_{23} may be assumed zero.

Other L-Auger measurements with poorer resolution have been made for Hg^{199} by Haynes and Achor[17] and for Ba^{137} by Burford and Haynes.[18] Rubenstein and Snyder[19] have calculated theoretical relative intensities of L-Auger lines of argon, krypton, and silver.

The above yields and all others which are known to have been published since Burhop's table are given in Table V. Again the agreement of subshell yields is not satisfactory, especially in the cases of a_2 and ω_2.

Whereas the transition probability for x-rays and roughly full-energy Auger electrons varies fairly smoothly from one element to another, the Coster-Kronig transitions, for example $L_1L_3M_5$, are energetically forbidden for certain elements and highly probable for neighboring elements. Thus it is difficult to predict from its neighbors what the subshell yields of an element will be and direct measurements are desirable. Therefore in view of the poor resolution of the work of Haynes and Achor and the lack of other work on Hg, a study of the high resolution spectrum of Hg was undertaken with Au^{199} used as the primary source.

The purpose of the L-Auger study was to: (1) determine the relative intensities of the L-Auger lines and line groups for Hg^{199}; (2) determine the total L-Auger and L-fluorescence yields for Hg^{199}; (3) obtain additional evidence for the values of subshell yields for high Z elements. The results of the L-Auger study are given in Sec. IVC.

II. APPARATUS

In order to achieve high resolution and good reliability at low-electron energies, a Moussa-Bellicard type double-focusing spectrometer[20] has been built at Vanderbilt University.[21] This instrument utilizes a $B/r^{\frac{1}{2}}$ field which is produced by the use of four pairs of suitably oriented coils, without using any ferromagnetic materials for field shaping. Thus, there is no residual magnetism to cause poor reliability at low energies. The coil arrangement used is similar to that of Moussa and Bellicard but the spectrometer proper has been completely re-engineered and has a 30-cm mean radius. Three pairs of Helmholtz type coils are used for compensating the earth's field. The instrument uses a continuous flow Geiger counter with very thin organic-film windows for particle detection.

Upon initial assembly and without adjustment the instrument was capable of a resolution of about 0.15%. The transmission could be increased at the expense of resolution.

The energy calibration of the instrument was obtained with the K-conversion electrons resulting from the decay of Cs^{137}.

The field control circuit of the spectrometer allows the magnetic rigidity (Br) to be varied from less than 70 gauss cm to 5665 gauss cm, corresponding to an energy range of less than 0.5 kev to 1.26 Mev. The upper range of energy may be increased to 1.97 Mev with a minor modification. The general outline of the field control system is described below and preliminary data are given.

The current for the focusing coils of the spectrometer is supplied by a $7\frac{1}{2}$ kw, 125 v General Electric motor-generator system. The commutator noise has been attenuated by incorporating the generator and focusing coils in the output of a negative-feedback amplifier system. The noise is thus attenuated by a factor equal to the loop transfer function of the system. Noise components of frequencies higher than those which can be passed by the generator itself are bypassed to the focusing coils through a cathode follower. The entire system is designed to satisfy the Nyquist criterion. The generator noise output is attenuated to better than 1 part in 10^4. The negative-feedback system is similar to that which has been employed by Sommers *et al.*[22]

The focusing field of the spectrometer is controlled by a double rotating coil system. One coil rotates in the field of the spectrometer and the other in the field of a thermo-stated permanent magnet used as a standard field. The two coils are mounted on a common shaft about 14 feet long, so as to get the permanent magnet, which is shielded, and drive motor well outside the spectrometer field. The system is rotated at 21.5 cycles per sec. The output of the coil rotating is the permanent magnet (standard field) is divided by a precision Dekavider, manufactured by Electro-measurements, Inc., then added out of phase to the signal produced by the coil rotating in the spectrometer. The error signal is amplified, phase detected, stabilized, and then fed into the noise reduction—generator circuit to complete the field feedback loop. The accuracy of control is better than 1 part in 10^4.

At present the control circuit is not automatic but steps are being taken toward complete automation.

III. EXPERIMENTAL PROCEDURE

The 3.15 day beta emitter Au^{199}, obtained from Oak Ridge National Laboratory, was used as the source to study the electron spectra of Hg^{199}. The beta decay of Au^{199} (Fig. 1) is complex[3] and contains three branches. One branch results in decay directly to the ground state of Hg^{199} while the other two leave the Hg^{199} in excited

[17] S. K. Haynes and W. T. Achor, J. phys. radium **16**, 635 (1955).
[18] A. O. Burford and S. K. Haynes, Bull. Am. Phys. Soc. Ser. II, **3**, 208 (1958).
[19] R. A. Rubenstein and J. N. Snyder (private communication) from J. N. Snyder, 1957.
[20] A. Moussa and J. B. Bellicard, J. phys. radium **15**, 85 (1954).
[21] Q. Baird, J. C. Nall, and S. K. Haynes, Bull. Am. Phys. Soc. Ser. II. **3**, 306 (1958).
[22] H. S. Sommers, P. R. Weiss, and W. Halpern, Rev. Sci. Instr. **22**, 612 (1951).

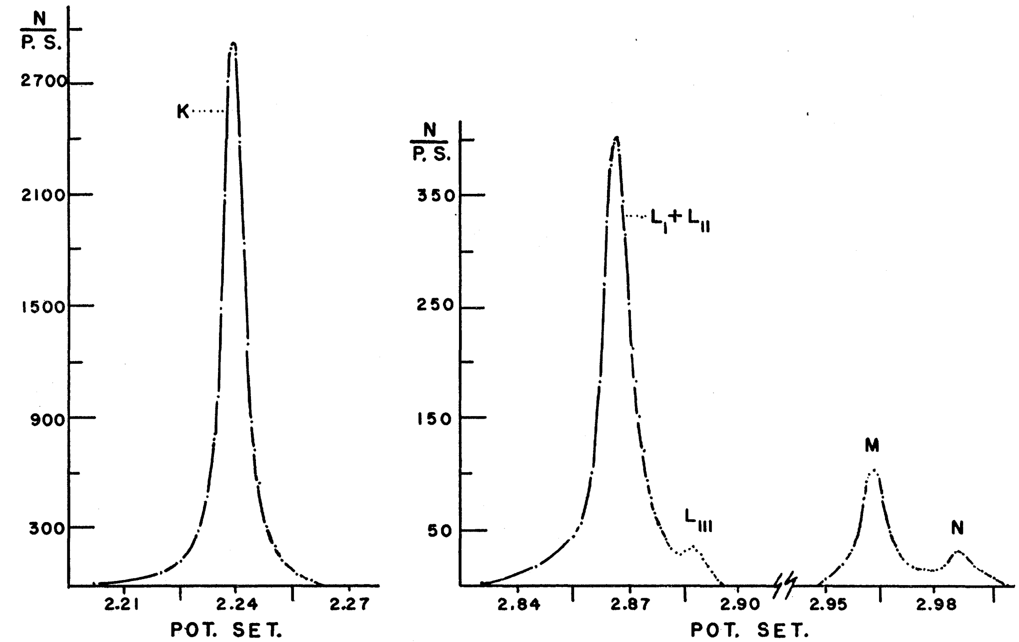

FIG. 2. Conversion lines of the 209-kev transition in Hg^{199}. Note. $L_{I}+L_{II}$ and L_{III} are the same notations as L_1+L_2 and L_3 in the text.

states. The de-excitation gamma rays, both cascade and cross over, are internally converted to form the primary vacancies for the Auger process. The Au^{199} was delivered in the form of chlorides in solution with dilute HCl. Since the half-life is so short, it was felt that thinner sources would be acquired if a re-extraction was carried out immediately before the source was evaporated. This would not only eliminate the Hg which was present from Au already decayed, but would remove other impurities. The activity was dried on a platinum filament and then standard source evaporation techniques were used to deposit a narrow, thin source of Au on a 10 $\mu g/cm^2$ Formvar film which had been made conducting by evaporating about 10 $\mu g/cm^2$ of Al onto it. Best results were obtained by pre-heating the filament. Then from this temperature the filament was "flashed" several times at about 1500°C for less than a second. This prevented damage to the thin source backing.

The techniques used produced sources which showed no thickness effects in the K Auger and conversion line region. However, in the L-Auger region there were thickness effects which decreased the effective resolution of the instrument.

For the detection of very low-energy electrons, very thin counter windows are necessary in order to obtain accurate intensity measurements. The windows for the work reported here were all made from collodion films supported on Lektromesh screens of various sizes. The data for the energy range 30 kev to 470 kev were taken with a 50 $\mu g/cm^2$ counter window and data below 30 kev were obtained with windows of 10 $\mu g/cm^2$.

The short half-life of the isotope used necessitated the use of several sources in order to obtain sufficient data. The data taken with the sources were collected during continuous operation of the spectrometer. Points were taken at intervals of 0.05% in momentum over the major peaks and other peaks of interest.

To obtain satisfactory statistics, at least 6000 raw counts per point were taken over most of the K-Auger region and many more than this on some of the high intensity conversion lines. About 3000 raw counts were collected at each point on the main L-Auger peaks. The spectrometer was operated with a momentum resolution of 0.30%, although source thickness considerably lowered the effective resolution in the L-Auger region. With this resolution the transmission was about 0.5%. A Magnatest Precision Field Meter was used periodically to insure that the compensating field was properly adjusted.

IV. RESULTS

A. Conversion Spectrum

The conversion spectrum consists of twelve groups and lines superimposed on the beta-ray continuum. Figures 2, 3, and 4 show these groups after subtraction of the continuum by Fermi-plot analysis. The relative intensity data, normalized to the 209-kev K line, are shown, together with those of other observers[2,3] in Table I. The intensities were determined by area measurements and the lines and groups were separated by graphical techniques. The 209-kev K line was used as an ideal line shape since it was well isolated in the spectrum.

In our spectrum the 159 L_1 and the 209 L_2 could be separated by line shape techniques but the uncertainties

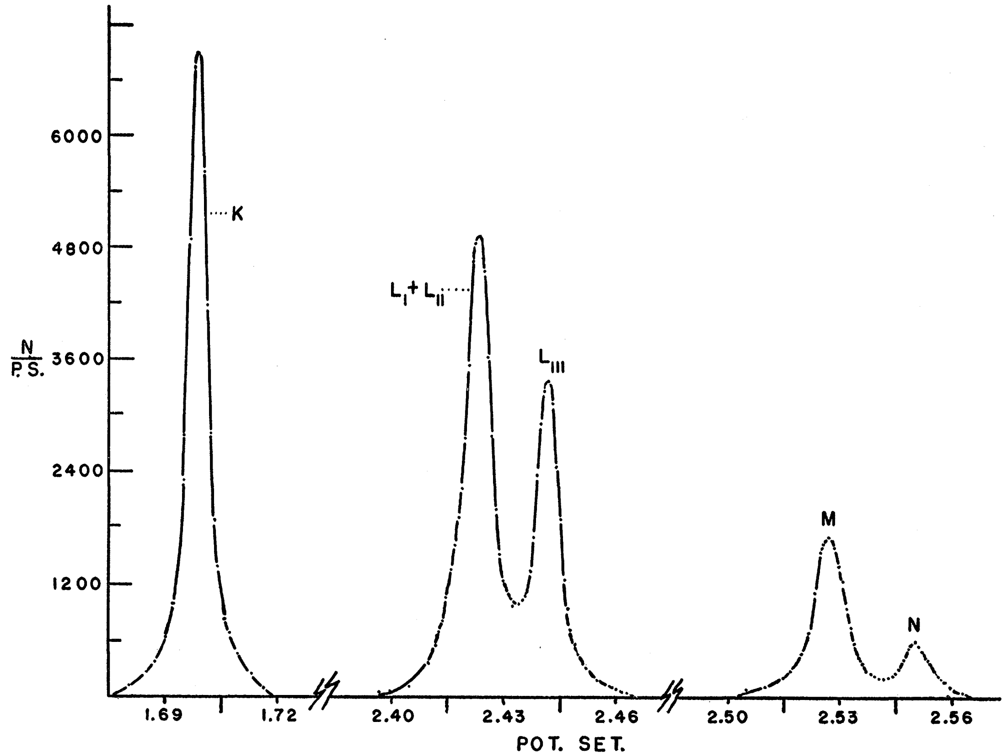

FIG. 3. Conversion lines of the 159-kev transition in Hg^{199}. Note. $L_{I}+L_{II}$ and L_{III} are the same notations as L_1+L_2 and L_3 in the text.

in intensities were so great that they are not listed separately in Table I.

For the 209-kev lines the agreement is excellent but serious discrepancies exist for both the 51- and 158-kev lines. With respect to the 51-kev line the agreement between NBH and CW is excellent except for the M shell, while BBB show a much lower L_1 intensity. We believe that this may have arisen from absorption by their counter window which had about a 6-kev cutoff and so might conceivably have appreciable absorption at 36 kev. We, therefore, adopt the NBH and CW values for the L_1 and L_2 shells and the average of all three as being more correct for the M shell.

TABLE I. Experimental intensities of the conversion lines for mercury-199.

Energy NBH[a] kev	Assign-ment	Relative intensity NBH[a]	CW[b]	BBB[c]	Most probable
35.2	51 L_1	0.429 ±0.011	0.428	0.267	0.429 ±0.01
35.8	51 L_2	0.038 ±0.002	0.037	0.033	0.037 ±0.002
37.8	51 L_3	0.005 ±0.0003		0.005	0.005 ±0.0003
46.6	51 M	0.120 ±0.010	0.077	0.077	0.091 ±0.02
49.4	51 N	0.029 ±0.002			0.029 ±0.002
50.1	51 O	0.007 ±0.0004			0.007 ±0.0004
75.9	158 K	1.932 ±0.060	1.990	1.458	1.961 ±0.04
125.9	209 K	1.000	1.000	1.000	1.000
144.5	158 L_1 }	1.957 ±0.054		0.243	0.282 ±0.03
145.1	158 L_2 }		1.761	1.417	1.63 ±0.05
147.1	158 L_3	1.140 ±0.034	1.250	1.033	1.15 ±0.03
156.3	158 M	0.834 ±0.03	0.801	0.700	0.82 ±0.03
158.9	158 $N+O$	0.218 ±0.009	0.205	0.200	0.21 ±0.01
194.7	209 L_1 }	0.178 ±0.005	0.156	0.155	0.155 ±0.005
195.4	209 L_2 }		0.031	0.028	0.029 ±0.003
197.2	209 L_3	0.0086 ±0.0003	0.0089	0.008	0.0085 ±0.0003
206.2	209 M	0.0429 ±0.008	0.0574		0.050 ±0.006
208.8	209 $N+O$	0.0146 ±0.005	0.0115		0.0130 ±0.004

[a] NBH—Nall, Baird, and Haynes.
[b] CW—Cressman and Wilkinson, see reference 2.
[c] BBB—Bäckström, Bergman, and Burde, see reference 3.

In the case of the 159-kev transition the disagreement is even more complex. The agreement between NBH and CW in K, total L, total M and $N+O$ is very good. The only substantial disagreement between these observers is in the L subshell intensities where the somewhat better line separation and more certain beta-ray background of NBH should make their results more dependable. We find it difficult to understand the large discrepancies in K, total L, and total M between these two observers and BBB. In addition to the mention by the latter of possible geiger counter instabilities, another possibility might be the fact that BBB did not make a complete Fermi-Kurie analysis as did NBH and CW. Nevertheless the L-subshell ratios of BBB appear to be quite accurate including particularly the L_1 intensity which they alone alone measure. We believe that the most accurate intensity ratios for the 158-kev transition are obtained by using the average of NBH and CW for the K, total L, M, $N+O$ coefficients, by using the average ratio $(L_1+L_2)/L_3$ from NBH and BBB and the ratio L_1/L_2 from BBB. These values are listed in the last column of Table I.

Since our results differ somewhat from CW and BBB, since new values of energy are available for the transitions,[4] and since Rose's Tables[7] have been published since their work, a complete recalculation of many of their final results seems in order.

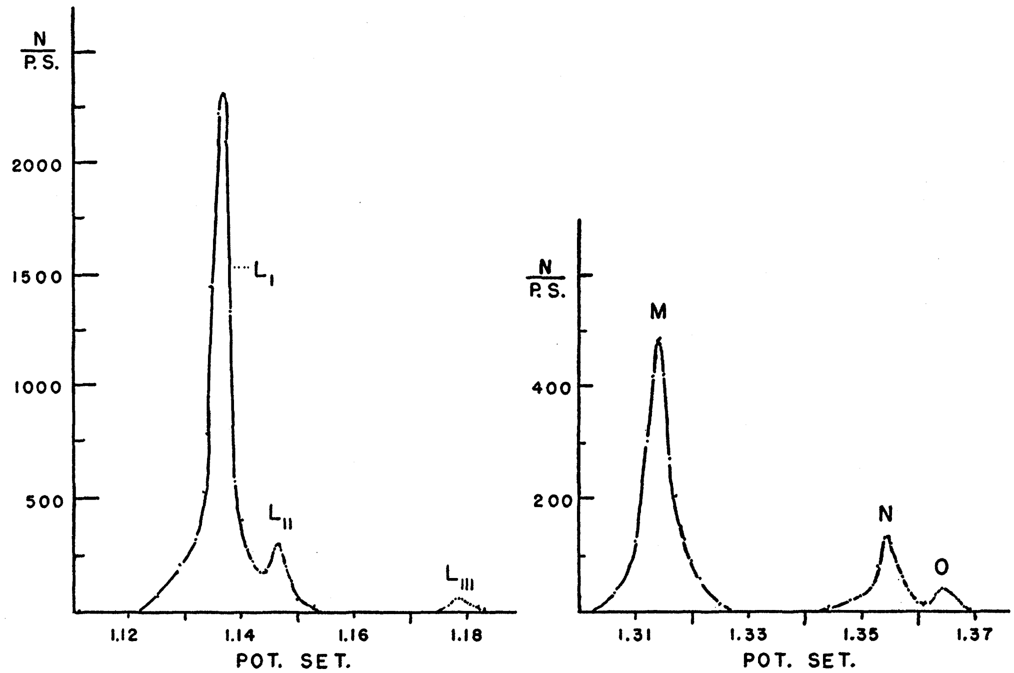

FIG. 4. Conversion lines of the 50-kev transition in Hg^{199}. Note. L_I, L_{II}, and L_{III} are the same notations as L_1, L_2 and L_3 in the text.

First, the pertinent conversion coefficients α_2 and β_1 were obtained by interpolation for each line from Rose's Tables and tabulated in the first two columns of Table II. The actual conversion coefficient for each line a_i ($i=k$, 1, 2, 3, M, N, 0) is related to α_{2i} and β_{1i} by the equation

$$a_i = r\alpha_{2i} + (1-r)\beta_{1i}, \quad (4)$$

where r is the fraction of the transitions which are $E2$. The a_i are related to the experimental intensities given in the last column of Table I (N_i) by

$$a_i = N_i/N_\gamma, \quad (5)$$

where N_γ is the gamma-ray intensity involved.

For the 51-kev transition the three L-subshell intensities give six equations and five unknowns. Thus two independent values of r are obtained (2.2×10^{-4} and 4.4×10^{-4}) which, when averaged give the value $(3.3\pm1)\times10^{-4}$. From Eq. (4) for L_1 a value of a_1 is obtained which is essentially independent of r. From this value of a_1 and Eq. (5) the most accurate value of N_γ is obtained. Subsequently the remaining values of a are obtained by repeated use of Eq. (5). The large discrepancy in the values of r and the value $a_2=0.592$ which is lower than either theoretical value (α_2 or β_1) indicates a discrepancy between relative peak intensities and Rose's relative values for β_1. The real problem is L_2 which is not completely resolved by NBH and CW

TABLE II. Average values of r and N_γ.

Conversion line (kev)	α_2	β_1	r	a_i	N_γ
51 L_1	0.86	6.86		6.86	$(6.25\pm0.2)\times10^{-2}$
52 L_2	47.0	0.668	$(3.3\pm1)\times10^{-4}$	0.592 ± 0.006	
51 L_3	48.6	0.0694		0.080 ± 0.006	
51 M				1.46 ± 0.3	
51 N				0.468 ± 0.04	
51 O				0.11 ± 0.01	
158 K	0.310				6.33 ± 0.1
209 K	0.154	0.843		0.723 ± 0.05	
158 L_1	0.037				7.62 ± 0.7
158 L_2	0.258				6.32 ± 0.2
158 L_3	0.180				6.39 ± 0.2
158 M				0.129 ± 0.05	
158 $N+O$				0.033 ± 0.02	
209 L_1	0.0200	0.117	0.113 ± 0.01	0.112 ± 0.005	
209 L_2	0.0750	0.0111		0.021 ± 0.003	1.383 ± 0.07
209 L_3	0.0462	0.00104		0.0061 ± 0.0004	
209 M				0.036 ± 0.004	
209 $N+O$				0.009 ± 0.003	

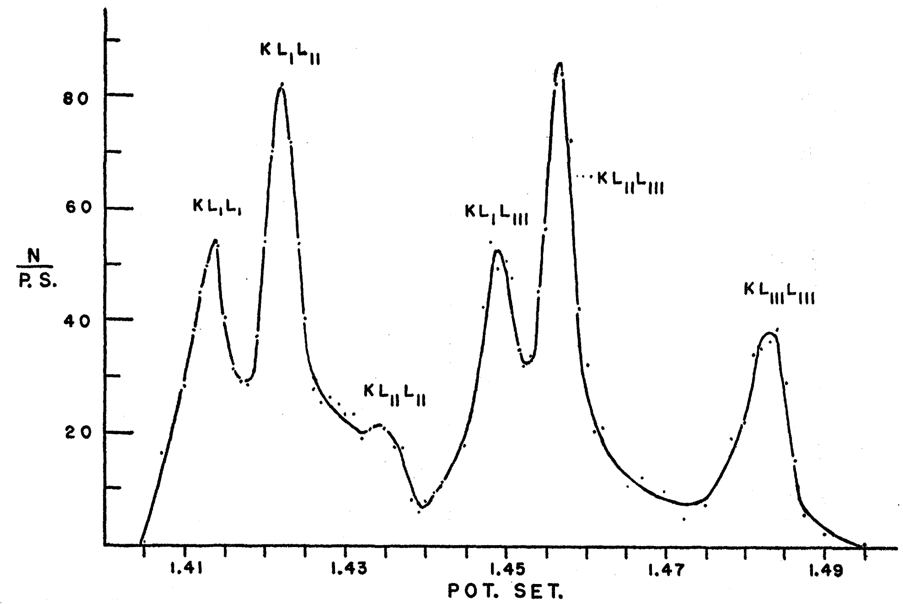

FIG. 5. The KLL-Auger spectrum of Hg^{199}. Note. $KL_{I}L_{I}$, $KL_{I}L_{II}$, $KL_{II}L_{II}$, $KL_{I}L_{III}$, $KL_{II}L_{III}$, and $KL_{III}L_{III}$ are the same notations as KL_1L_1, KL_1L_2, KL_2L_2, KL_1L_3, KL_2L_3, and KL_3L_3 in the text.

and probably suffers some window absorption in BBB. It is probable that the measured value of this line is at least 10 to 15% too low.

The 158-kev transition is treated as a pure $E2$ transition ($r=1$) and N_γ is calculated for each line. With the exception of the L_1 line which is only partially resolved by BBB the agreement is excellent. This substantiates both the $E2$ assignment and the relative values of Rose's K, L_2, and L_3 conversion coefficients for an $E2$ transition of this energy. By use of the average value of N_γ (6.35±0.1) and Eq. (5) the remaining a_i were calculated.

The 209-kev transition was handled similarly to the 51-kev transition except that equations for K, L_1, and L_3 (L_2 being too inaccurate) were used to determine r and N_γ. The agreement between the two values is satisfactory for both. The averages are given in Table II. The values of a_i are calculated from the average value of N_γ and Eq. (5).

The satisfactory internal consistency of the calculations on the 209-kev transition (K, L_1, and L_3 levels) indicates satisfactory agreement between Rose's coefficients (α_2 and β_1) and the relative line intensities of Table I. A further and more absolute check of the accuracy of the theoretical conversion coefficients is obtained by the agreement between $N_\gamma^{158}/N_\gamma^{209}$ as calculated above by use of Rose's coefficients, 4.59 ±0.23, and the directly measured value of Cressman and Wilkinson[2] 4.53±0.23.

Finally, the total intensities of the three transitions are 0.51 kev, 0.646±0.03, 158 kev, 12.40±0.1, and 209 kev, 2.639±0.14. From these intensities, the ratio of the 251-kev beta group to the 302-kev group is found to be 0.280±0.015. If the 460-kev branching ratio of 6.4% is taken from Haynes and Achor[17] the branching ratios of the lower energy transitions are (251 kev) (20.4±1)% and (302 kev) (73.2±1)%. As indicated by Bäckström *et al.*, these values are probably more accurate than those directly measured from the beta-ray spectrum 24.3%, and 69.3%.

B. K-Auger Spectrum

The K-Auger spectrum is shown in Figs. 5 and 6. To calculate the total or global K-Auger yield it is only necessary to measure the total area under the Auger lines and compare it with the area of the two K-conversion lines. The measured yield for Hg^{199} is $a_K=0.048\pm0.003$. This value is in agreement with a value obtained previously by Broyles *et al.*,[23] and yields a value for the fluorescence yield that falls on the semiempirical curve of ω_K versus Z that has been worked out by Burhop.[24] It should be pointed out that the

TABLE III. Comparison of experimental and theoretical KL_xL_y intensities for mercury.[a]

Line	Energy (kev)	Theor.[b,c]	Theor.[d,e]	Exp.[f]	Exp.[g]
KL_1L_1	53.56	1.00	1.00	1.00	1.000
KL_1L_2	54.19	1.02	1.2	1.2	1.323±0.1
KL_1L_3	56.15	1.65	2.27	0.70	0.853±0.06
KL_2L_2	55.07	0.23	0.15	0.20	0.401±0.03
KL_2L_3	56.73	1.46	4.32	1.40	1.279±0.08
KL_3L_3	58.70	0.81	2.40	0.60	0.760±0.05

[a] See footnote reference 31.
[b] R. D. Hill (see reference 26).
[c] Calculated as internal conversion of x-rays.
[d] W. N. Asaad and E. H. S. Burhop, Proc. Phys. Soc. **71**, 369 (1958).
[e] Calculated with nonrelativistic theory using intermediate coupling.
[f] I. Bergström and R. D. Hill, Arkiv Fysik **8**, 21 (1954).
[g] Present work.

[23] C. D. Broyles, D. A. Thomas, and S. K. Haynes, Phys. Rev. **89**, 715 (1953).
[24] E. H. S. Burhop, J. phys. radium **16**, 624 (1955).

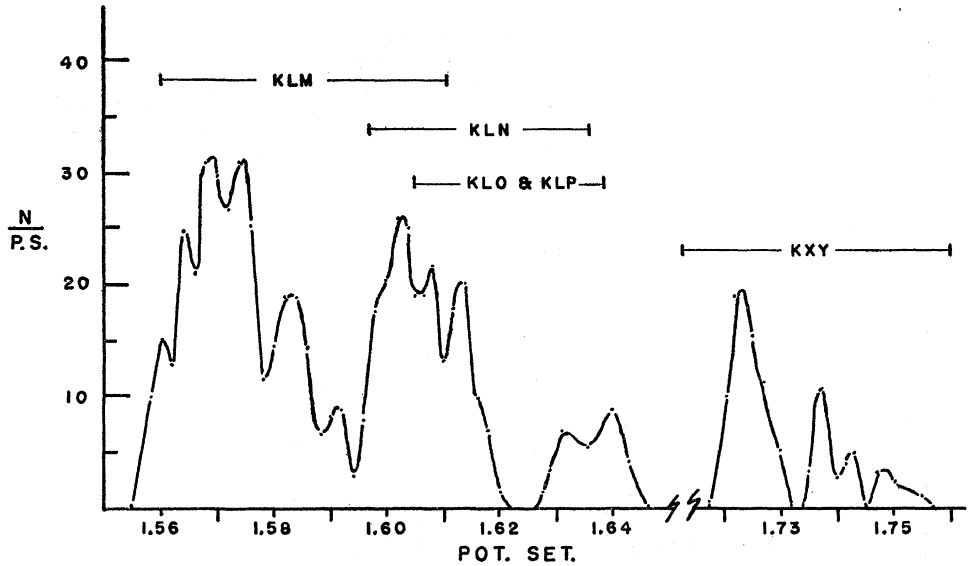

FIG. 6. The KLX- and KXY-Auger spectra of Hg^{199}.

present value is a factor of three more precise than the previous value. The ratios of the KLL lines to the KLX and KXY are also quantities of interest in comparing experiment to theory. These are measured as $KLL:KLX:KXY::1.000:0.496\pm0.015:0.094 \pm0.003$. These values are in sharp disagreement with those previously obtained by Broyles *et al.*, but follow the general empirical Z dependence trend demonstrated by Bergström[25] who used previous data covering a spread in Z from 29 to 81. It is possible to separate the individual KL_xL_y lines by use of an ideal line shape, and to account for all of the area of the KL_xL_y spectrum. The energies, assignments and relative intensities are shown in Table III. Previously determined values are shown in the same table, as well as theoretical values. The present experimental findings have relatively good overall agreement with the previous measurements and agree quite closely with some of the theoretical calculations made by Hill.[26]

Separations of some parts of the structure of the KLX-Auger group are possible but only three constituent lines can be completely separated from adjacent lines. The intensities of these components and the group assignments are shown in Table IV

TABLE IV. Relative intensities of KLX Auger groups for mercury.

Energy (kev)	Relative intensity	Assignments
64.6	1.00	KL_1M_1
64.9	1.23	KL_1M_2
65.3	2.14	KL_2M_1, KL_1M_3, KL_2M_2
65.9	2.14	KL_1M_4, KL_1M_5, KL_2M_3
66.4	2.42	KL_2M_4, KL_2M_5
67.1	0.45	KL_3M_1
67.6	1.15	KL_3M_2, $KL_1N_{1,2,3}$, $KL_1N_{4,5}$
68.0	1.98	KL_3M_3, $KL_2N_{1,2,3}$, $KL_1N_{6,7}$ KL_1O, KL_1P
68.4	1.10	$KL_2N_{4,5}$, KL_3M_4
68.8	2.09	KL_3M_5, $KL_2N_{6,7}$, KL_2O, KL_2P
70.5	0.86	KL_3N_{1-7}
71.1	0.75	KL_3O, KL_3P
...	3.31	KXY

[25] I. Bergström in *Beta- and Gamma-Ray Spectroscopy*, edited by K. Siegbahn, (North-Holland Publishing Company, Amsterdam, 1955), Chap. XX, p. 633.

C. L-Auger Spectrum

The data in the L-Auger region are plotted in Fig. 7. The beta background is positioned by use of points on the continuum on each side of the L region. The Fermi plot was not utilized because in the region below 45 kev there was an upward deviation of the plot of the lowest energy beta-ray group. In view of the straightness of the Fermi plot of Haynes and Achor[17] to less than 20 kev, this upward deviation is undoubtedly due to source thickness.

Separating the various lines in the L-Auger spectrum is a major problem. In the short range of less than 10 kev, there are 45 lines from the LMM group, 105 from the LMN, and 84 from the LNN, with the many additional weak ones from the LXY. Because of source thickness and possibly back scattering, a fair amount of low-energy "tailing" in the L region is observed. Thus the standard line shape of the upper energy range cannot be used here for line separation. Also the "tailing" noticeably increases in going from the high to the low-energy end of the L-Auger spectrum. Therefore, even if a standard line is available it must be varied in shape with change in energy. The $L_3M_2M_3$ line (peak 3) is selected as a first approximation to the standard line at the low-energy end and the $L_2M_2M_3$ line (peak 7) is used for the middle region. Peak 3 is well removed from neighboring lines but source thick-

[26] R. D. Hill, Phys. Rev. **91** 770 (1953).

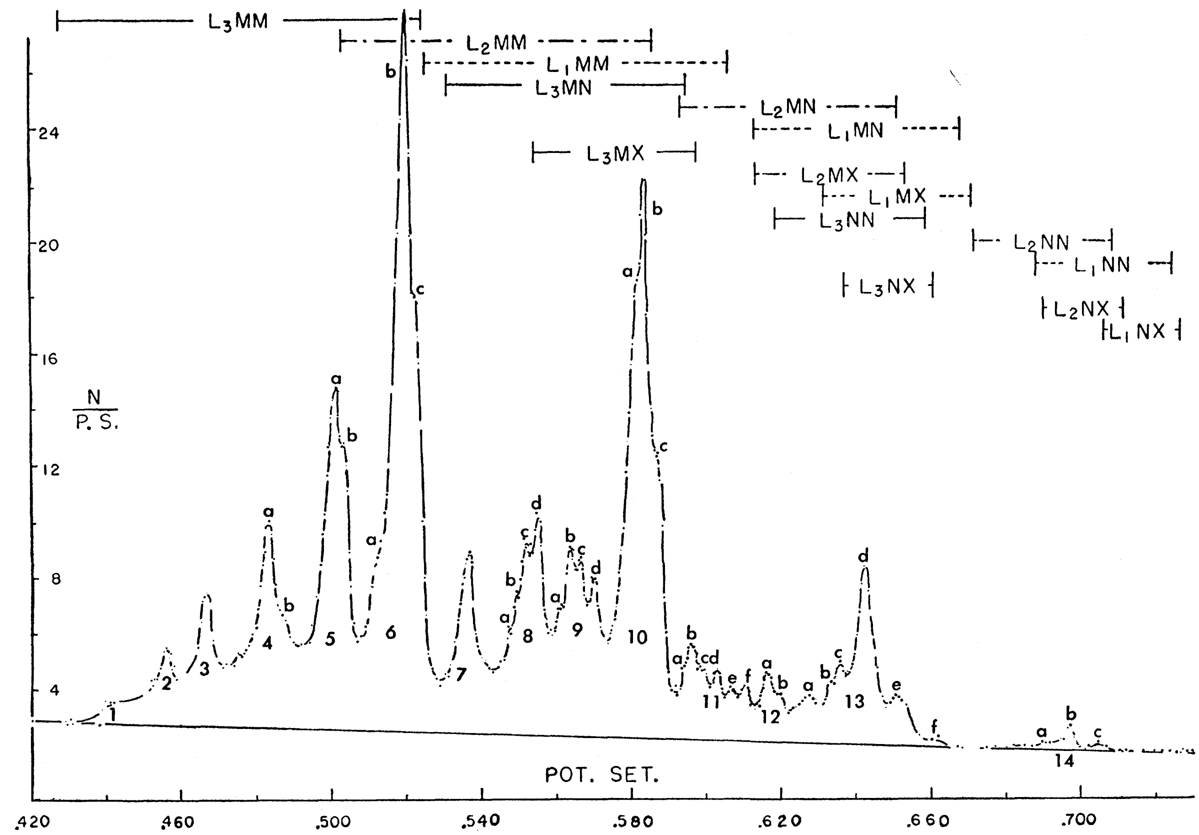

FIG. 7. The L-Auger spectrum of Hg^{199}.

ness causes the effective line width to be about 1.3% in this region. Peak 7 shows no structure, so it is assumed that the neighboring line $L_1M_1M_2$ makes no contribution. The adjacent line $L_3M_1N_1$ is assumed to be insignificant in strength. The line width of peak 7 is about 1.0%. Since no isolated line is available in the higher energy end of the spectrum, an approximation was made by extrapolating the shapes of the two lower ones. The effective line width in the upper region is about 0.5% or better. By use of these line shapes, the spectrum is graphically divided into its component lines and line groups. The peaks are designated on the basis of energy calculations.

Additional peak separation is obtained by assuming internal consistency. For example, the configuration $L_2M_{45}N_{45}$ (peak 13d) is very strong relative to most other L_2 peaks. It seems reasonable that $L_3M_{45}N_{45}$ should also be strong since L_2 and L_3 differ only in spin-orbit orientation and the remainder of the electrons involved in these composite lines have all possible combinations of spin-orbit orientation. As a result, a large fraction of the intensity of line 10c is assigned to $L_3M_{45}M_{45}$. Consequently, $L_2M_5M_5$ is far weaker than $L_2M_4M_4$, whereas $L_3M_5M_5$ is far stronger than $L_3M_4M_4$, a contrast which also seems reasonable. Use is also made of the theoretical results of Rubenstein and Snyder[19] for silver where no other guidelines exist.

Finally our assignments within each of the three bands ($L_1L_2L_3$) have been compared in intensity with those of Sujkowski and Slätis[27] (SS) and Geoffrain and Nadeau[28] (GN) for a composite source (from ThB) of Tl^{208} and Bi^{212}. The resolution of SS was far superior to ours so that the identification of their observed lines is reasonably certain. They observed some lines which we do not because of higher resolution, but missed some faint ones due to photographic insensitivity which we observed. Our agreement with the semiquantitative intensity scale of SS is on the whole excellent and in particular seems to justify most of our line splitups based on internal consistency. Our agreement with GN is far poorer as is the agreement between SS and GN. Although the resolution of GN is superior to ours, it does not seem to have been sufficiently so to overcome the difficulty of the overlapping spectra of Tl^{208} and Bi^{212}.

The relative intensities are presented in Table V. The main columns of intensities are fairly accurate but the further subdivisions indicated in parentheses are approximations and may be in error. Since in most cases

[27] Z. Sujkowski and H. Slätis, Arkiv Fysik **14**, 101 (1958).
[28] C. Geoffrion and G. Nadeau, Can. J. Phys. **35**, 1284 (1957).

they do not involve major lines these approximations do not affect greatly the conclusions given below.

As a side line to the intensity determinations, the ratios of LMM:LMX:LXY (where X and Y are N and above) are measured and found to be 1.00:0.30 ±0.03:0.016±0.004. These ratios are the counterparts of KLL:KLX:KXY which are often measured in K-Auger work except that in the L-Auger case the ratios are also functions of the mode of excitation.

The next step in the analysis of the data from the L-Auger region is that leading to the determination of the total and subshell yields for Hg^{199}. Initial L vacancies for Hg^{199} must first be known. These result from: (1) L conversion; (2) KLL-Auger ejection (produces two vacancies per Auger event); (3) KLX-Auger ejection; (4) KL x rays. The L conversion and KLL-KLX-Auger vacancies, both total and subshell, are taken directly from the high-energy part of the present work. The

TABLE V. Relative intensities of L subshell lines.[a]

Peak	Designation	Rel. int. (percent)	
1	$L_3M_1M_2$	1	(?)
	$L_3M_2M_2$		
2	$L_3M_1M_3$	1.5	
3	$L_3M_2M_3$	4.0	
4a	$L_3M_3M_3$	6.45	
	$L_3M_2M_4$		
4b	$L_3M_2M_5$	0.76	
5a	$L_3M_3M_4$	5.6	
5b	$L_3M_3M_5$	5.7	
6a	$L_3M_4M_4$	2.1	
6b	$L_3M_4M_5$	11.0	
6c	$L_3M_5M_5$	9.1	(8.6)
	$L_2M_2M_2$		(0.5)
7	$L_2M_2M_3$	5.0	
8a	$L_3M_2N_2$	0.33	
8b	$L_3M_2N_3$	0.96	(0.66)
	$L_1M_1M_3$		(0.3)
8c	$L_2M_3M_3$	1.7	
	$L_2M_2M_4$		
8d	$L_2M_2M_5$	4.0	(2.4)
	$L_3M_2N_{45}$		(1.6)
9a	$L_3M_3N_2$	0.59	
9b	$L_3M_3N_3$	2.1	(1.7)
	$L_1M_1M_4$		(0.4)
9c	$L_2M_3M_4$	2.6	(2.2)
	$L_1M_1M_5$		(0.4)
9d	$L_2M_3M_5$	3.0	(1.0)
	$L_3M_3N_{45}$		(1.4)
	$L_3M_{45}N_{12}$		(0.4)
	$L_1M_2M_4$		(0.2)
10a	$L_2M_4M_4$	6.1	(4.4)
	$L_3M_{45}N_3$		(1.5)
	$L_1M_2M_5$		(0.2)
10b	$L_2M_4M_5$	7.2	
10c	$L_2M_5M_5$	6.3	(1.5)
	$L_3M_{45}N_{45}$		(4.3)
	$L_1M_3M_{45}$		(0.5)
11a	$L_3M_4N_{67}$	0.26	
11b	$L_3M_5N_{67}$	1.3	
11c	$L_1M_4M_4$	0.62	
11d	$L_1M_4M_5$	0.81	
11e	$L_2M_2N_2$	0.47	(0.3)
	$L_1M_5M_5$		(0.2)
11f	$L_2M_2N_3$	0.78	
12a	$L_2M_2N_{45}$	1.0	
	$L_2M_1N_{67}$		
	$L_2M_3N_1$		
12b	$L_2M_3N_2$	0.67	
	$L_2M_3N_3$		
13a	$L_2M_3N_{45}$	1.1	
	$L_2M_4N_1$		
13b	$L_2M_{45}N_{12}$	0.66	(0.5)
	$L_3N_3N_3$		(0.2)
13c	$L_2M_{45}N_3$	0.95	
13d	$L_2M_{45}N_{45}$	3.8	(3.4)
	$L_3N_{45}N_{45}$		(0.4)
13e	$L_2M_{45}N_{67}$	1.4	(1.2)
	$L_3N_{45}N_{67}$		(0.2)
13f	$L_3N_{67}N_{67}$	0.14	
14a	L_2	0.15	
14b	$L_2N_{45}N_{45}$	0.27	
14c	$L_2N_{45}N_{67}$	0.1	

[a] Values in parentheses result from the use of various assumptions (Sec. IVC).

TABLE VI. Experimental L Auger, fluorescence, and Coster-Kronig yields determined since publication of table by Burhop (see reference 9).[a]

	ω_1	ω_2	ω_3	a_1	a_2	a_3	f_{12}	f_{13}	$f_{12}+f_{13}$	f_{23}	IC ex. ω_L	IC ex. a_L	EC ex. ω_L	EC ex. a_L
Ag(47)													0.029[m]	0.971[m]
Xe(54)													0.10[m]	0.90[m]
Ba(56)				0.324[h]	(0.485−0.629)[h]	0.946[h]			0.577[h]	(0.272−0.416)[h]				
					0.577[k]	0.658[k]					0.371[k]	0.629[k]		
Hg(80)	0.10[b]	0.32±0.03[g]	0.393[b]	0.16±0.02[g]	0.46±0.04[g]	0.607[g]		0.5[b]	0.74±0.04[g]	0.22±0.04[g]	0.410±0.04[g]	0.590±0.04[g]	0.24[m]	0.76[m]
Tl(81)	0.09[c]	0.66[c]	0.46[c]	0.15[i]	0.34[i]	0.54[i]	0.24[i]	0.52[i]	0.76[i]	0[ib]	0.50[i]	0.50[i]		
											0.68[l]	0.32[l]		
(81,83)				0.07±0.02[j]	0.46±0.09[j]	0.59±0.05[g]								
												0.52[j]	Fl. ex. ω_L	Fl. ex. a_L
Bi(83)	0.12[d]	0.32[d]	0.40[d]	0.11[d]	0.62[d]	0.60[d]	0.19[d]	0.58[d]	0.77[d]	0.06[d]	(0.38−0.49)[d]	(0.51−0.62)[d]	(0.39−0.56)[d]	(0.44−0.61)[d]
	0.11[e]	0.32[e]	0.34[e]	0.11[e]	0.68[e]	0.66[e]	0.16[e]	0.62[e]	0.78[e]	0[eb]	(0.30±0.05)[m]	(0.70±0.05)[m]		
	0.09[c]	0.66[c]	0.46[c]	0.15[i]	0.34[i]	0.54[i]	0.24[i]	0.52[i]	0.76[i]	0[ib]	0.37[e]	0.63[e]		
	0.11[f]		0.33[f]	0.07[f]	0.49[f]	0.67[f]	0.12[f]	0.70[f]	0.82[f]		0.38[n]	0.62[n]		
											0.49[i]	0.51[i]		
											0.68[l]	0.32[l]		

[a] See footnote reference 31.
[b] Values assumed from other work.
[c] Calculated from Burde and Cohen.
[d] (RaD) A. S. Ross *et al.* (see reference 10).
[e] (RaD) J. Tousset and A. Moussa (see reference 13).
[f] B. B. Kinsey, Can. J. Research **A26**, 421 (1948).
[g] Present work.
[h] A. O. Burford and S. K. Haynes (see reference 18).
[i] J. Burde and S. G. Cohen (see reference 16).
[j] K. Risch, Z. Physik. 150, 96 (1958).
[k] S. K. Haynes and W. T. Achor (see reference 17).
[l] A. Moussa and J. B. Bellicard (ThB) (see reference 14).
[m] B. L. Robinson and R. W. Fink, Revs. Modern Phys. **27**, 424 (1955).
[n] (RaD) N. Lee, thesis, Vanderbilt University, 1958 (unpublished).

contribution of KL x rays, both total and subshell, are calculated from the data of Beckman[29] and the total K-fluorescence yield from the present work. The relative number of L-Auger electrons emitted is measured by a planimeter in the standard manner. The total L-Auger yield for Hg is found to be 0.590 ± 0.04, thus the total fluorescence yield is 0.410 ± 0.04. This is in good agreement with the value of Auger yield (0.629 ± 0.035) reported by Haynes and Achor.[17]

To calculate subshell yields, Eqs. (1) (2), and (3) must be supplemented by three additional equations which incorporate quantities measured by the spectrometer.

$$a_1=A_1/n_1, \tag{6}$$

$$a_2=A_2/(n_2+f_{12}n_1), \tag{7}$$

$$a_3=A_3/[n_3+f_{13}n_1+f_{23}(n_2+f_{12}n_1)], \tag{8}$$

where: A_i is the total number of L_i-Auger electrons (non-Coster-Kronig) per K-conversion event, and n_i is the number of initial (non-Coster-Kronig) vacancies in the L_i subshell per K-conversion event.

Of the 15 quantities in Eqs. (1) to (3) and (6) to (8), (A_i's and n_i's) are known from spectrometer measurements. Three of the other nine must be taken from other sources. As may be seen from the table of Tousset and Moussa,[12] there is good agreement among recent investigators (Ross *et al.*,[10] Burde and Cohen,[16] and Tousset and Moussa[18]) for the value of ω_1 for Bi. Substantiating evidence for the value of ω_1 comes from the value given by Kinsey.[30] The values of ω_2 and a_2 reported by Burde and Cohen are in violent disagreement with those reported by Ross *et al.*, and Tousset and Moussa. The values for ω_3 given by Burde and Cohen, and Ross *et al.*, are in reasonably good agreement. The disagreements among the three groups of investigators do not seem too large in the case of the Coster-Kronig yields. The terms accepted from previous work, or arbitrarily, were ω_1, ω_3, and f_{13} for Bi ($Z=83$).

The value of ω_1 was estimated for Hg by extrapolation from Kinsey's[30] value of ω_1 for Bi ($\omega_1=0.10$). Burhop's formula[26] was used to extrapolate the value of ω_3 for Bi to that for Hg ($\omega_3=0.393$). While the agreement on f_{12} and f_{13} by other investigators is only fairly good (Table VI), the influence of these parameters on Eqs. (7) and (8) is not very great because of the small value of $n_1(0.27)$. Furthermore, examination of Eq. (8) shows that if f_{23} is assumed small, the value of f_{13} must be of the order of unity or greater. Since this is, if not impossible, at least in violent disagreement with the results of other investigators given in Table VI, it follows that our data and interpretation are clearly inconsistent with $f_{23}\approx0$.

Because of the insensitivity of Eqs. (7) and (8) to the values of f_{12} and f_{13}, any reasonable choice of the values of f_{12} and f_{13} should give fairly accurate values for a_2, ω_2, and f_{23}. In view of this fact it is assumed that f_{13} has a value of 0.5.

By using only the data from the present spectrometer measurements it is found from Eq. (6) that $a_1=0.16\pm0.02$. With the values of ω_1, ω_3, and f_{13} determined from previous work, it follows from use of Eqs. (3), (1), (7), (8), and (2) in the order given that: $a_2=0.46\pm0.04$; $f_{23}=0.22\pm0.04$; $\omega_2=0.32\pm0.03$ (See Table VI).

Since f_{12} is very sensitive to the value selected for f_{13} therefore no value of f_{12} is quoted. However a fairly accurate value for $f_{12}+f_{13}$ is found directly from Eq. (1) to be $f_{12}+f_{13}=0.74\pm0.04$.

V. ACKNOWLEDGMENTS

It is a pleasure for the authors to acknowledge two grants from the National Science Foundation which made it financially possible to construct and operate the spectrometer. Thanks are also due L. Fincher, who designed and supervised the construction of the compensating coils and to R. A. Parker, who designed and tested the counter. The efficient data taking of N. Lee, H. Boyd, J. Brediger, and B. Curry was invaluable.[31]

[29] O. Beckman, Phys. Rev. **109**, 1950 (1958).

[30] B. B. Kinsey, Can. J. Research **26**, 404 (1948).

[31] Three references relating to Table III and Table VI either had not appeared or were missed. Table III: The recent theoretical results of W. N. Asaad, Proc. Roy. Soc. (London) **249**, 555 (1959) should be added to Table III. His relativistic calculations (*j-j* coupling) give $KL_1L_1=1.00$, $KL_1L_2=1.44$, $KL_1L_3=0.82$, $KL_2L_2=0.09$, $KL_2L_3=1.46$, and $KL_3L_3=0.66$.

Table VI: Additional results for ω_L are given in R. W. Fink, Phys. Rev. **106**, 271 (1957), and B. L. Robinson and R. W. Fink, Revs. Modern Phys. **32**, 127 (1960).